

Received 17 January 2023, accepted 26 February 2023, date of publication 6 March 2023, date of current version 10 March 2023.

Digital Object Identifier 10.1109/ACCESS.2023.3253290

RESEARCH ARTICLE

Monitoring and Assessment of SBAS-InSAR Deformation for Sustainable Development of Closed Mining Areas—a Case of Nanzhuang Mining Area

ZHEN LI^{1,2}, ZHONGBIN TIAN², BIN WANG², WEIBING LI³,
QIHAO CHEN⁴, AND ZHENGJIA ZHANG⁴

¹School of Resources and Geosciences, China University of Mining and Technology, Xuzhou 221116, China

²Coal Geological Geophysical Exploration Surveying and Mapping Institute of Shanxi Province, Jinzhong 030600, China

³Shanxi Coal Geological Investigation and Research Institute Company Ltd., Taiyuan 030000, China

⁴School of Geography and Information Engineering, China University of Geosciences, Wuhan 430078, China


Corresponding author: Zhengjia Zhang (zhangzj@cug.edu.cn)

ABSTRACT Closed mining areas are an important potential resource, and rational use of them are critical to implementing sustainable development strategies. To guide the more reasonable development and utilization of the closed mining areas, we proposed a method of surface deformation monitoring and subsidence risk assessment of the closed mining areas with SBAS-InSAR technology. Based on the analysis of deformation, a risk assessment model integrating subsidence hazard and subsidence vulnerability was proposed. Subsidence hazard include accumulate deformation and the subsidence rate of the last year. The tunnels and the land use types are used to assess the subsidence vulnerability. This method can achieve deformation monitoring and risk assessment of the closed mining areas, and the proposed method is validated by taking the Nanzhuang mining areas as an example. The results showed that the main subsidence areas in the closed mining areas are located in the tunnel in the southwest and the gangue pile area in the northeast of the mining areas, while the deformation in the vegetation-rich forested area is low. The area of low, medium and high subsidence risk zones is 65.5%, 27.8% and 6.7% respectively.

INDEX TERMS Closed mining area, SBAS-InSAR, subsidence risk assessment, deformation monitoring.

I. INTRODUCTION

As the earth's resources are strained, the need for sustainable development is growing [1]. Among them, coal resources are continuously mined as an important energy source for industrial development, and the number of closed mines is gradually increasing [2], [3]. With the increase in the number of closed mines, the demand for research on resource utilization of closed mines has gradually increased, and the subsidence of closed mines will have an impact on the resource development and utilization of closed mines. The research usually focuses on the subsidence changes of coal mines in mining

The associate editor coordinating the review of this manuscript and approving it for publication was Geng-Ming Jiang .

and ignore the subsidence changes in the closed mining areas. Due to the long-term and hidden nature of the ground deformation evolution in the mining areas, the closed mining area can also cause a series of hazards, such as ground cracks or cave-ins [4], posing great threaten to people's productivity and life. According to the China Coal Industry Association annual report, China has closed 5500 coal mines by the end of 2020. [5]. The continuous deformation monitoring of closed mining areas and the assessment of subsidence risk can provide important basis for the management and sustainable development and utilization of closed mining areas [6].

The monitoring methods for ground subsidence in closed mining areas are still mainly based on traditional methods such as level surveying and global positioning system

(GPS) [7], [8]. Although the traditional geodetic method can accurately measure the deformation at point scale, the method have obvious limitation, such as small monitoring coverage and high cost of human and material resources [9]. Interferometric Synthetic Aperture Radar (InSAR) is a remote sensing method capable of dynamic ground deformation monitoring with the advantage of large scale, high resolution, and high accuracy [10], [11]. With the development of Multi-Temporal InSAR (MT-InSAR) technology [12], [13], [14], [15], [16], shortcomings (temporal decorrelation and atmospheric delay) of traditional InSAR methods have been overcome [17], [18], [19], [20], [21]. The two popular MT-InSAR methods are persistent scatterer InSAR (PS-InSAR) and small subset InSAR (SBAS-InSAR). PS-InSAR is more suitable for areas with more permanent scatterer distribution such as urban areas, and SBAS-InSAR is more suitable for areas with more distributed targets such as mining areas [22].

The SBAS method was utilized to monitor the ground motion in the South Wales coalfield, UK, and to analyze the correlation between ground uplift changes and groundwater before and after mine closure in 2014 [23]. Li et al. used a time-series InSAR approach to monitor the deformation of the northwest suburban coalfield in Xuzhou from 2015 to 2020 and discovered that the coal mine closure time influenced the surface deformation by analyzing three modes: mine subsidence, subsidence-uplift, and subsidence-uplift-subsidence [24]. Chen et al. used the SBAS-InSAR technique to obtain the surface deformation of the mine closure after 5 years. The results showed that the maximum subsidence rate in the study area was -43 mm/yr in five years, and the accumulated maximum subsidence was 310 mm, which exceeded the safety threshold range of buildings and required continuous monitoring [25].

The SBAS-InSAR technique has been widely used for monitoring deformation in mine closure areas, and scholars have analyzed the deformation results accordingly. However, the research usually focuses on the relationship between subsidence and subsurface elements (groundwater, etc.), and there is a lack of research on the relationship between subsidence and surface land use types, as well as the assessment of subsidence risk in closed mining areas [26], [27], [28]. The subsidence monitoring analysis and risk assessment of the closed mining areas can help the comprehensive utilization of the closed mine resources and promote sustainable development.

Therefore, the objective of this paper is to monitor and assess of ground deformation in closed mining area using SBAS-InSAR. Based on the ground deformation, we have assessed the subsidence risk of the closed mining area. The closed Nanzhuang mine in Yangquan, Shanxi Province was taken as the study area. 104 Sentinel-1A images acquired from January 8, 2018, to June 21, 2021, were selected for time-series deformation monitoring of the mining areas. Furthermore, the spatial and temporal subsidence feature before and after the closure of the Nanzhuang mining areas have

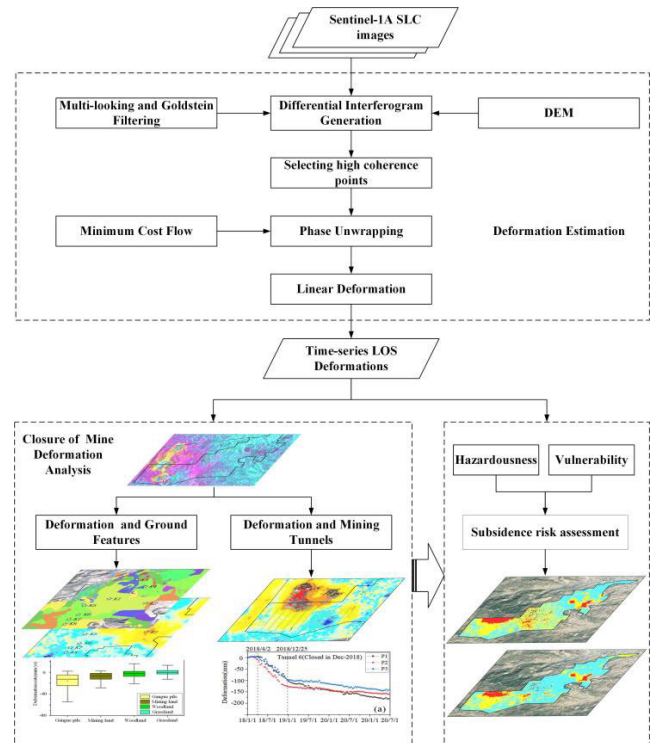


FIGURE 1. Flow chart of subsidence risk assessment of the closed mining areas.

been explored. The relationship between internal mine tunnels, surface land use types and ground subsidence have been analyzed.

II. METHODS

The method of this paper is mainly divided into three parts: deformation estimation of the closed mining areas, subsidence analysis of closed mining areas, and subsidence risk assessment of closed mining areas. In this paper, the SBAS-InSAR method is used to estimate the subsidence results of the closed mining areas, and the subsidence characteristic are analyzed from the perspectives of tunnel closure time, surface feature type of the closed mining areas, etc. The subsidence risk assessment system is proposed separately according to the characteristics of the closed mining areas. Figure 1. shows the main steps of the method.

A. DEFORMATION ESTIMATION

The SBAS method was proposed in 2002 [29], [30]. In this study, we obtained the deformations by the SBAS-InSAR. The specific steps to obtain the deformation of the closed mine site are as follows.

The Sentinel-1A image on January 22, 2020 is selected as the super master image, whereas the others are secondary images. The selection of interferograms is constrained by a maximum spatial baseline of 150m and a maximum temporal baseline of 50 days. The signal-to-noise ratio is improved by performing multi-looking factors of 4×1 in the range and

azimuth directions, along with the Goldstein filtering method. The minimum cost flow (MCF) network is used for phase unwrapping [31]. We set the coherence threshold of 0.2 to improve the accuracy [32]. Then, the interferometric pairs with poor unwrapping (The interferogram contains obvious atmospheric phase or there are many areas with low coherence coefficients) and low coherence are eliminated.

After phase unwrapping, 20 Ground Control Points (GCPs) are selected to correct the unwrapped phase. A polynomial model was used to mitigate the phase components caused by residual orbital errors and long-wave atmospheric delay. Preliminary displacements are estimated by a robust and commonly used linear model [33]. Meanwhile, the residual topography is also removed. Then, the atmospheric phase was removed by atmospheric filtering. Subsequently, geocoding in the line of sight (LOS) direction is used to calculate deformation. Finally, the subsidence rate and time-series subsidence are obtained and mapped across the study area.

B. DEFORMATION ANALYSIS

Whether the mine environment is stable and safe is directly attributable to the sustainable development and utilization of the closed mining areas. This paper analyzes the relationship between SBAS-InSAR deformation results of the closed mining areas and surface land use types, tunnel closure time, etc. On this basis, further risk assessment of the closed mining areas is carried out to better guide the development and utilization of the closed mining areas.

1)Deformation and different ground features: Explore the relationship between surface subsidence and surface land use types (Land use type sources were manually interpreted and field surveyed) in closed mining areas, for example, make a comparative analysis of surface subsidence in gangue piles, mining area and other areas, and study whether there are some rules in the subsidence of different land use types.

2)Deformation and mining tunnels: Combined with the mining tunnel data, the temporal and spatial analysis of mining subsidence is carried out to explore the deformation evolution characteristic after the closure of the tunnel. Explore the influence of different closing time of tunnel on surface subsidence. Meanwhile, the influence of adjacent mining area on the subsidence of closed mining area is analyzed.

C. SUBSIDENCE RISK ASSESSMENT

According to the expression proposed by the United Nations Humanitarian Affairs: Riskiness = Hazardousness * Vulnerability (ISDR 2002). That is, the risk of a specific region at a specific time is composed of the degree of danger in the region at this time and the ability of the region to resist the risk (the degree of suffering dangerous losses). This paper determines the relevant risk assessment system by combining the available information with the mine closure and referencing the urban risk assessment system 2020 [34].

Comprehensive hazard and vulnerability to obtain risk assessment, and then divided into three levels of risk: high

TABLE 1. The weight and scores of hazard indexes.

Hazard indexes	Weight	Levels Criteria	Scores
Accumulate Subsidence(mm)	0.5	<50	1
		50~200	2
		>200	3
Subsidence Rate of The Last Year(mm/yr)	0.5	<10	1
		10~30	2
		>30	3

TABLE 2. The weight and scores of vulnerability indexes.

Vulnerability indexes	Levels Criteria	Scores
Land-use Types	Nature Land (woodland, Grassland, etc.)	1
	Agricultural Land	2
	Industrial Land	2
	Residential-Office Land	3
Tunnels	Closed tunnels	2

risk area, medium risk area and low risk area. The risk calculation formula is as follows:

$$R = \sum_{i=1}^n w_i * H_i * V$$

where R is the subsidence risk, i is the hazard indicator, w_i is the weight corresponding to hazard indicator i, H_i is the score corresponding to hazard indicator i, and V is the score indicating the vulnerability of the corresponding study area.

To visually describe the risk of the closed mining area, this paper uses hierarchical analysis to score and weight the hazard of subsidence and vulnerability to subsidence. The classification is divided into 3 levels, with scores of 1, 2 and 3 [35]. The specific indicators are shown in Table 1 and Table 2.

III. STUDY AREA AND DATASETS

A. STUDY AREA

The study area is the Nanzhuang mining area in Yangquan City, while the mine closure time is around December 2020. The location of the study area is shown in the red box in Figure 2(a). The Nanzhuang mine site is located about 3 km south of Yangquan City, in the area of Nanzhuang village, Yijing town, Yangquan suburb, to Lianghu village, Yexi town, Pingding county, and the location of the mining area in Yangquan is shown in Figure 2(a). The geographical coordinates are 37°47' 40–37°50' 40”N, 113°30' 50–113°35' 20”E.

The mining area is located on the western side of the central Taihang Mountains, in the hilly mountainous region in the eastern part of the Shanxi Plateau. Sedimentary stratigraphy within the mining area includes Ordovician, Carboniferous, Permian and Quaternary. The Lower Diodian Shanxi Formation and the Upper Carboniferous Taiyuan Formation are the

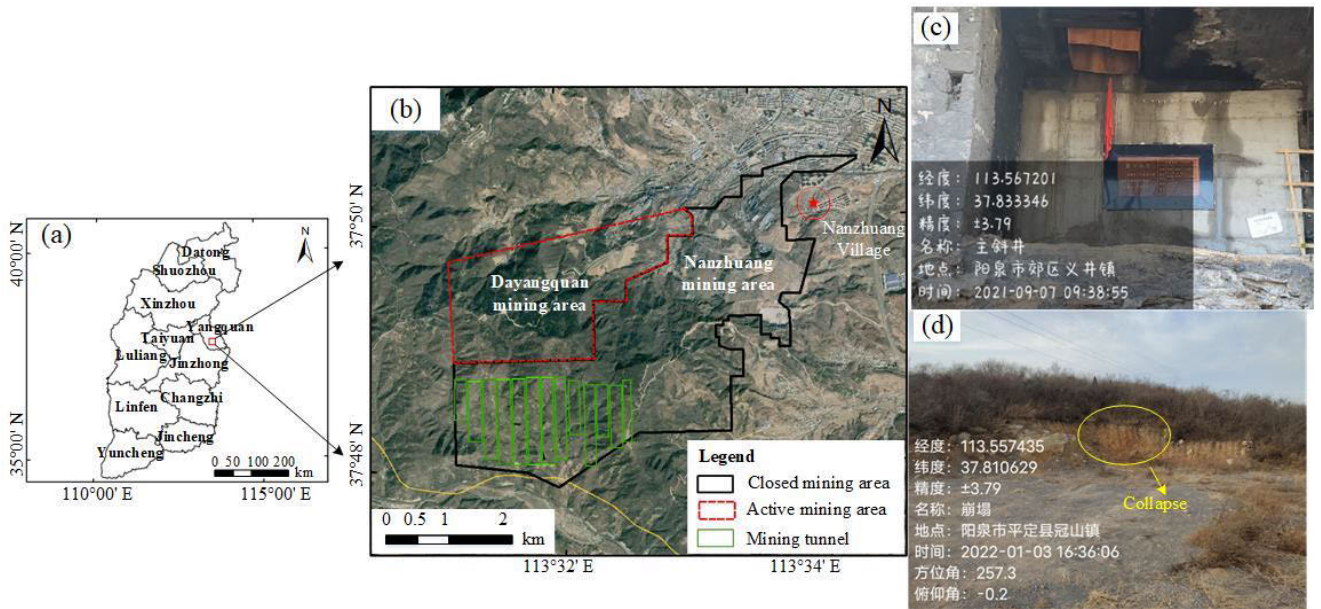


FIGURE 2. (a)The location of Yangquan Nanzhuang Mine; (b) The distribution of the closed mining area, active mining and mining tunnel. The background map is the optical image; (c) The main inclined shaft in Yijing town on the outskirts of Yangquan city (Longitude:113.567201°, Latitude:37.833346°, Precision: ±3.79, name: main slant shaft); (d) Yangquan City Pingding County Guanshan town collapse (Longitude:113.557435°, Latitude:37.810629°, Precision: ±3.79, name: Collapse, Azimuth: 257.3°, Pitch angle: -0.2°).

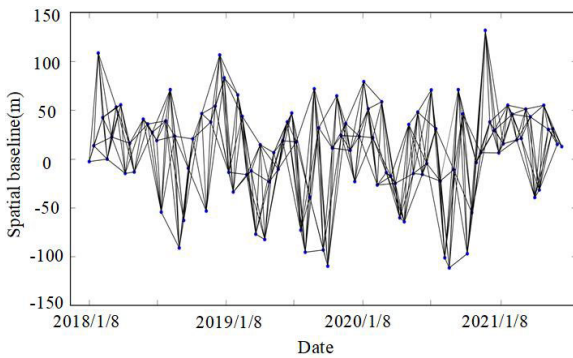


FIGURE 3. Temporal-spatial baselines of sentinel-1 images interferometric pairs.

main coal-bearing strata. The optical images of the location of the mining area are shown in Figure 2(b).

B. SAR DATASETS

The experiment selected 104 views of ascending orbit Sentinel-1A satellite SAR images covering the Nanzhuang mining area from January 8, 2018, to June 21, 2021. The images’ temporal-spatial baselines are shown in Figure 3. The Sentinel-1 satellite is an Earth observation satellite in the European Space Agency’s Copernicus program (GMES), comprising two satellites carrying a C-band synthetic aperture radar that can overcome various weather conditions and provide continuous images.

The data type is Interferometric Wide swath (IW) and Single Look Complex (SLC) at C-band with a wavelength

of 5.6 cm, a spatial resolution of 5 m × 20 m, and a polarization mode of VV polarization. The IW mode is the primary acquisition mode over land and fulfills most of the operational requirements. It acquires 250 km of data in the range direction. The IW mode captures three sub-regions using progressive scan SAR (TOPSAR) topographic observations. In TOPSAR technology, the beam can be electronically controlled from backward to forward in the azimuthal direction of each burst in addition to controlling the range of the beam such as a scanning radar, thus avoiding scalloping and resulting in uniform image quality over the entire area.

To remove the topographic phase from the original interferograms, the Shuttle Radar Topography Mission (SRTM) Digital Elevation Model (DEM) data with 30 m resolution were collected.

IV. EXPERIMENTAL RESULTS AND ANALYSIS

A. DIFFERENTIAL INTERFEROGRAMS

When the surface deformation occurs, two or more interferometric measurements are made by the SAR system for various periods in the same area to obtain the surface deformation, and this technique is called the D-InSAR technology [36]. The problems of temporal decoherence, DEM error, orbital error, atmospheric delay, and deconvolution error faced by D-InSAR results limit its further application. Figure 4 shows that the interferometric phase of different secondary images differs greatly, while the interferometric phase information is clearer and more accurate for short time bases. The red area is the area of the significant subsidence.

To overcome these problems, this paper adopts the SBAS-InSAR technique for mine deformation monitoring.

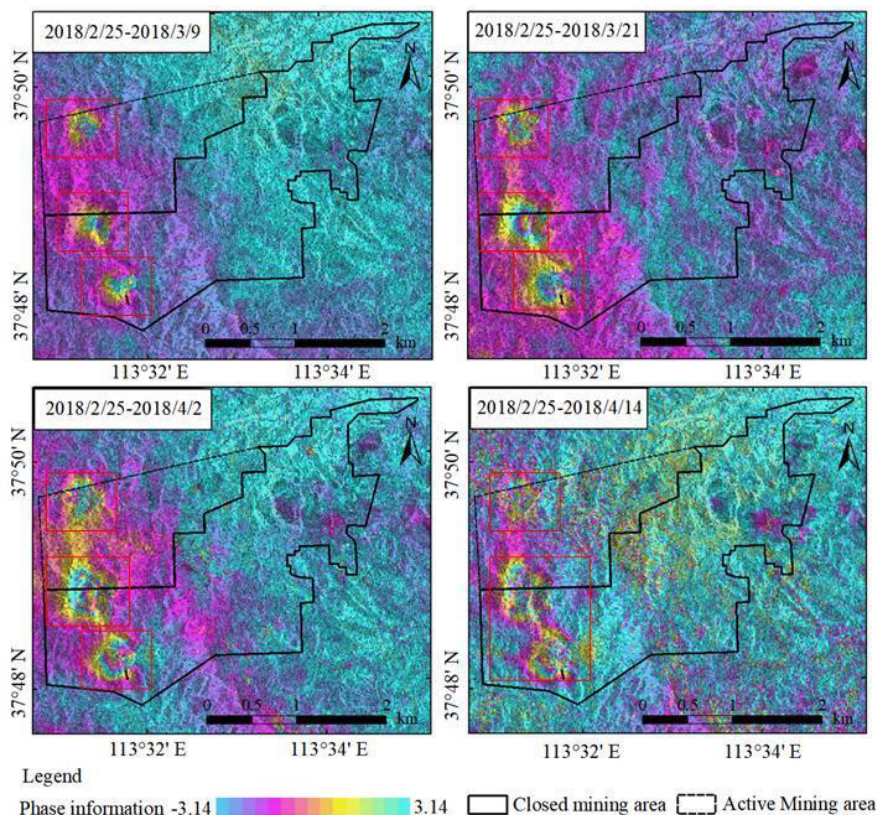


FIGURE 4. Differential interferograms maps with different temporal baseline (The area in red box is the area of significant subsidence).

B. DEFORMATION RESULTS

The average deformation rate results (Figure 5) and accumulative time-series deformation results (Figure 6) were finally obtained from January 8, 2018, to June 21, 2021, from the closed mining area in Nanzhuang, Yangquan, Shanxi Province, by the SBAS-InSAR method.

From Figure 5, most areas’ subsidence rate is between -10 mm/yr and 10 mm/yr within the mining area, because the coal mine has been closed. However, the external mining area of Dayangquan has a greater impact on the northern area of Lianghu village in the southwest corner of the Nanzhuang mine, while the overall maximum subsidence rate at the Dayangquan mining area is over -171 mm/yr. The internal area of the Nanzhuang mine is affected by the Dayangquan mine, while the maximum subsidence rate can reach -63 mm/yr. Inside the closed mining areas of Nanzhuang, the gangue pile located in the east of Shenyu village and the mining area have a larger average annual deformation rate, while the maximum deformation rate can reach -50 mm/yr or more.

Figure 6 shows that most of the regions have small deformation between -10 mm and 10 mm during the observation time, while the maximum subsidence in the local area is over -375 mm. Subsidence in the inner area of the Nanzhuang mine is primarily concentrated in the southwest tunnel area

and in the northeast gangue pile and mining area of the mine. In the south-west area of the closed mining areas of Nanzhuang, the maximum cumulative subsidence to the closed tunnels in recent years can reach over -150 mm, the previously closed tunnel had lifted, with the maximum cumulative lift not exceeding 30 mm. In the north-eastern zone of closed mining areas, the maximum accumulated subsidence of the gangue pile can reach more than -200 mm. As Figures 5 and 6 can be seen, the subsidence larger areas still need to be continuously monitored.

C. SUBSIDENCE RISK ASSESSMENT

From Figure 7, Figure8, the gangue pile area within the Nanzhuang mine and the area near the mining areas of the Dayangquan mine have a higher hazard of subsidence, and the total area of the closed mining is 11.86 km², with 9.8% of the high-hazard area, 41.8% of the medium-hazard area and 48.4% of the low-risk area, so it is necessary to carry out continuous deformation monitoring for the closed mining. The high-risk areas are mainly concentrated in the vicinity of the gangue pile in the northeast area within the mine and in the area bordering the closed mining and the northern mining Central Dayangquan mine, which still need continuous monitoring in the future. The area of high-risk area accounts for

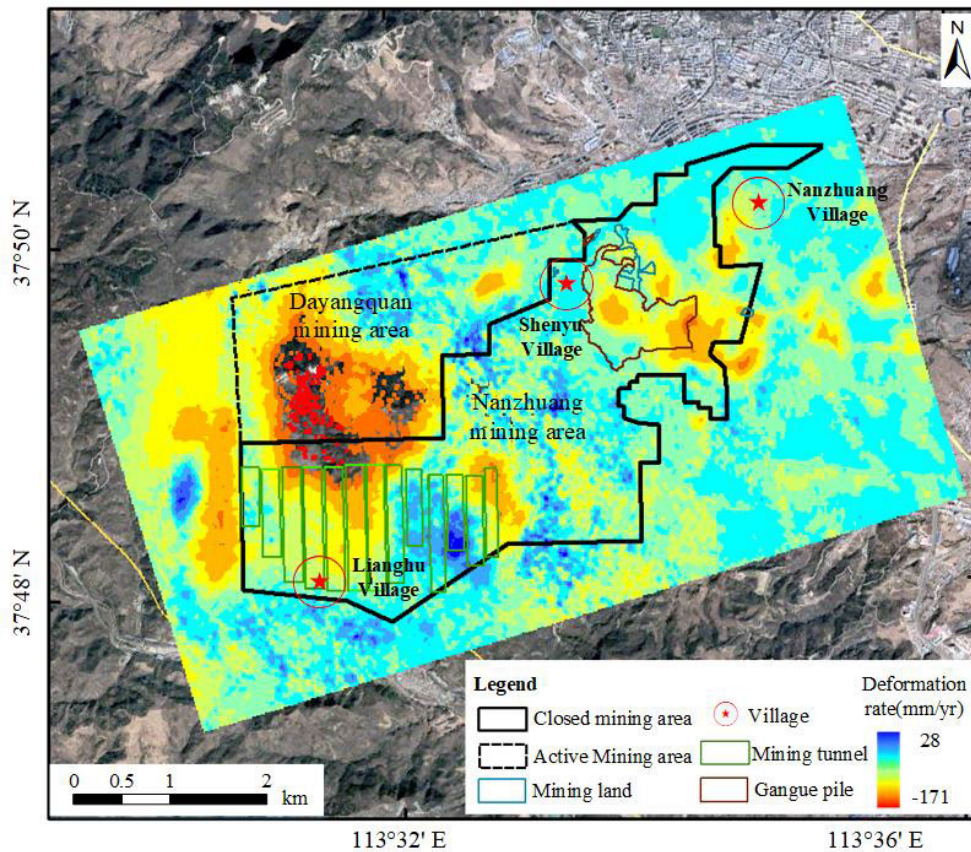


FIGURE 5. The LOS deformation rate map of Nanzhuang mine. (The star indicates the village, the black solid line indicates the closed mining area, and the black dotted line indicates the mining area under mining).

6.7%, the area of medium-risk area accounts for 27.8%, and the area of low-risk area accounts for 65.5%.

Note that the part of the Nanzhuang mining area has large gradient deformation under the influence of the mined area, the immediately adjacent Dayangquan mine, which is beyond the SBAS-InSAR monitoring capability. The deformation rate and cumulative deformation are not available for this part of the area, which is defined as a high-risk area in this paper.

D. VALIDATION AND LIMITATION

From Figures 5 and 6, the estimated deformation is mainly located inside the Dayangquan mine and the Nanzhuang mine where nearby the Dayangquan mine. This is consistent with the fact that the Dayangquan mining area is a mining area and the deformation should be large, while the Nanzhuang mining area is a closed mining area and the deformation should be small. Meanwhile, we obtained the photos from Nanzhuang village near the mine boundary (Figure 2(c) and Figure 2(d)). There is a potential collapse area in the upper right corner of the Nanzhuang collapse area in Figure 5, which is consistent with the monitoring results.

There are some limitations in this study: 1). The subsidence center of Nanzhuang mine is missing, which is due to its proximity to the mining area, Dayangquan mine. The deformation

of the subsidence center is so large that beyond the monitoring capacity of SBAS-InSAR, which can be further inverted by combing GPS, offset-tracking, etc. 2). From Figure 11, Figure 12, tunnel 13 has a short closing time, large subsidence, and errors in unwrapping. Therefore, the tunnel 13 time series deformation fluctuates more.

V. DISCUSSION

Subsidence in the closed mining areas is an important factor in subsidence risk assessment, so it is necessary to explore the subsidence characteristic in the closed mining areas. This paper investigated the characteristic of subsidence with the tunnel and the surface land use types in the closed mining area. The closed tunnel area of Nanzhuang mine and the area with rich land use types in the northeastern part of Nanzhuang mine were selected to determine the subsidence of each area according to the subsidence feature points, and the causes of subsidence were analyzed with the help of remote sensing images. And the spatial and temporal deformation trend of the tunnel area were analyzed.

A. DEFORMATION AND DIFFERENT GROUND FEATURES

This section focuses on the relationship between surface subsidence and land use types within the closed mining area.

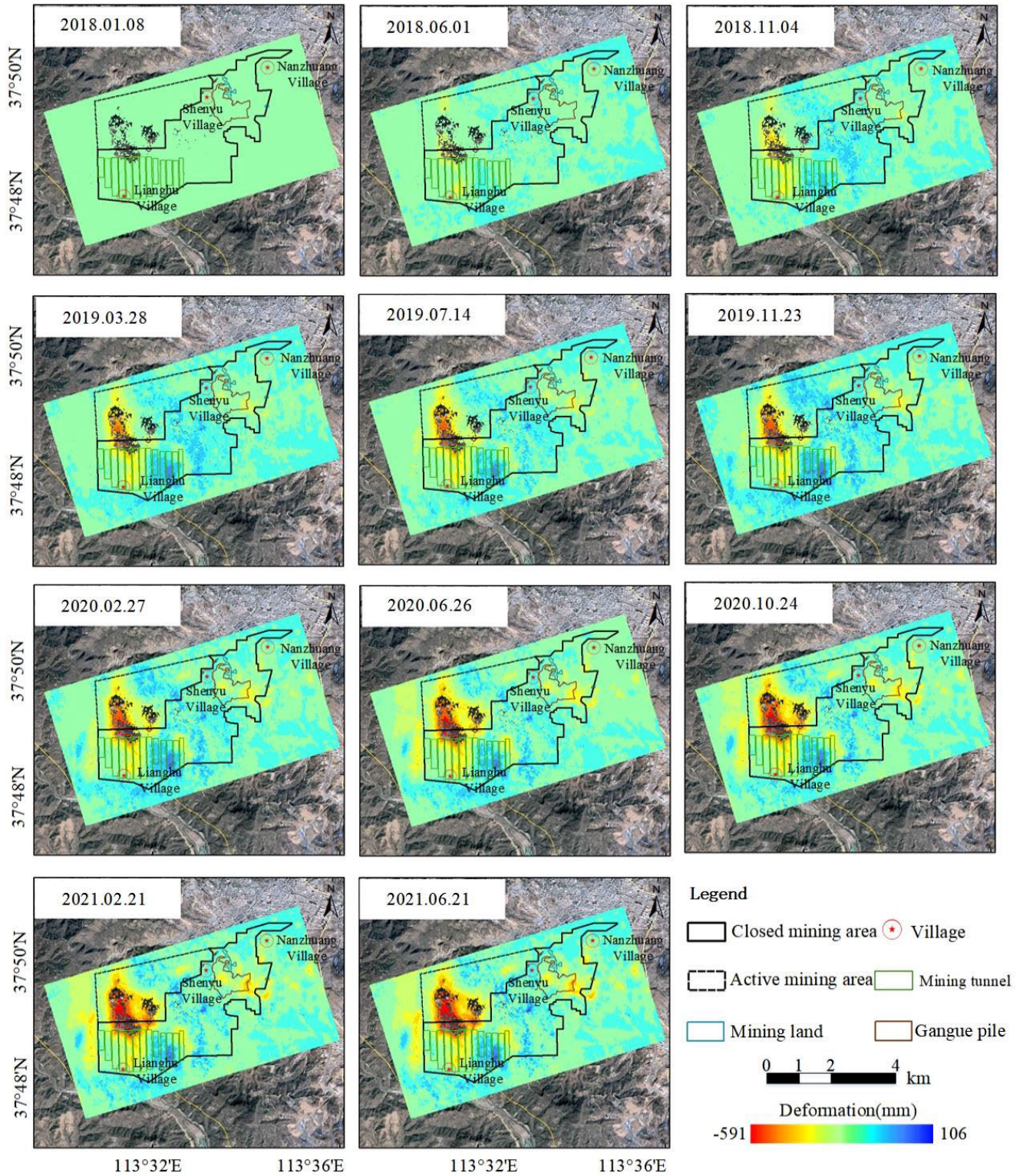


FIGURE 6. Nanzhuang mine LOS cumulative time-series deformation change map.

The northeastern area within the Nanzhuang mine near the subsidence is rich in land use types, as Figure 8(b) shown. Eight points, named K1 to K8, were selected for temporal

analysis of different land use types, respectively, where K1 and K2 were distributed on gangue pile, K3 and K4 were selected on mining area, K5 and K6 were selected on other

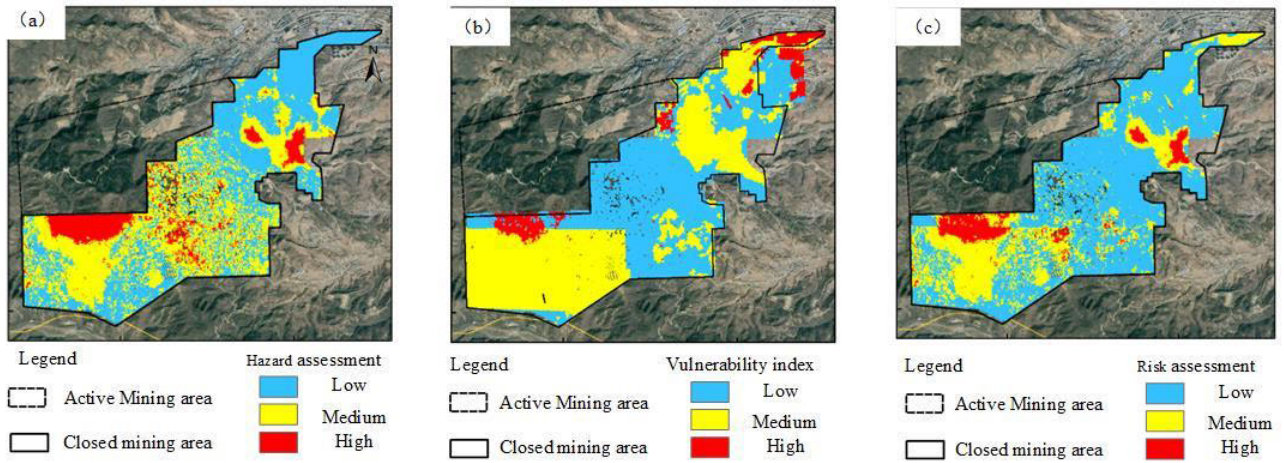


FIGURE 7. (a) Mine closure hazard assessment map, (b) Mine closure vulnerability index map, (c) Mine closure risk assessment map.

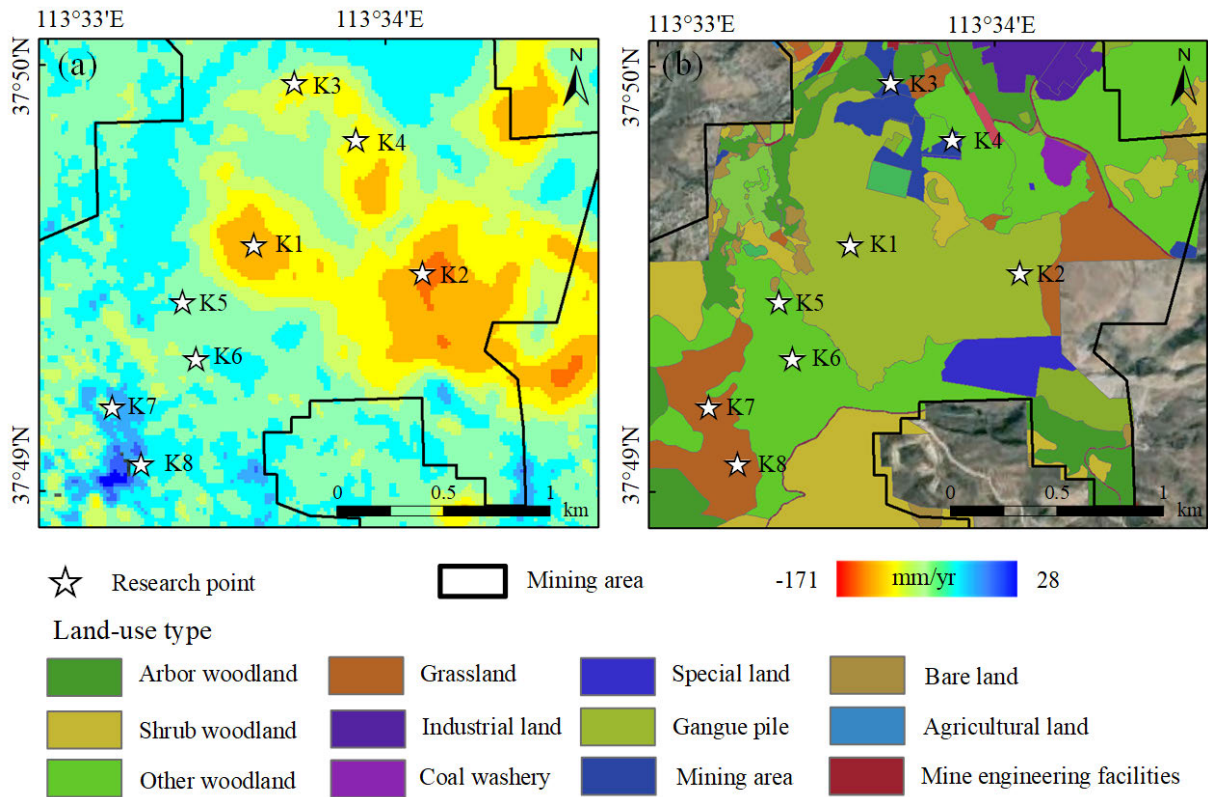


FIGURE 8. Deformation map and land-use type map of Nanzhuang mining areas (a) Deformation rate map of the northeastern region within the Nanzhuang mine, (b) Classification of land-use types within the Nanzhuang mine.

woodlands, and K7 and K8 were selected on grasslands. Figure 8(a) shows the deformation rate of the northeast area of the Nanzhuang mine, while several obvious subsidence funnels can be found. Figure 9 shows the time-series deformation for each specific point.

It can be seen from Figure 9 that the deformation of points K1, K2 located in the gangue pile is larger, the cumulative subsidence amount reached -128 mm and -197 mm, respec-

tively. The large deformation of the gangue pile is caused by mining activities artificial for the transport of the pestle. The other four points are woodland and grassland areas, which are more stable and have no obvious subsidence.

For the four land use types mentioned above, the deformation rate box line diagrams are shown in Figure 10. The deformation is more concentrated in the gangue pile and mining area, while the deformation of woodland and grassland

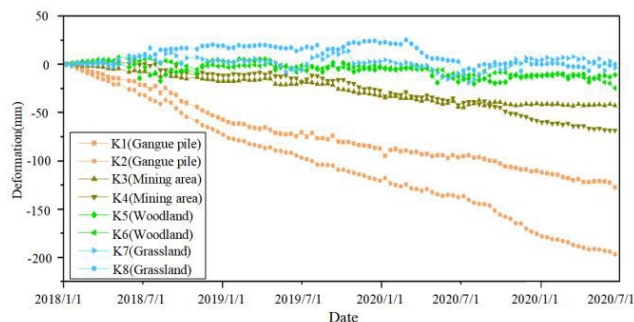


FIGURE 9. Time-series accumulated deformation map of points K1-K8.

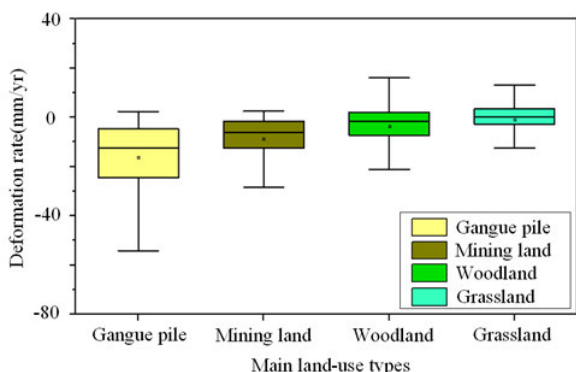


FIGURE 10. The box line diagram of the deformation rate distribution of different land-use types.

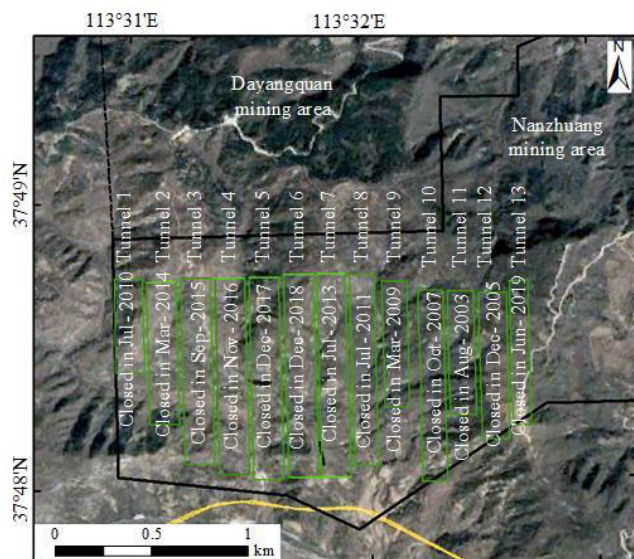


FIGURE 11. Optical image of Nanzhuang mine and the closed time of tunnels.

are smaller. The deformation rate of the gangue pile from -54.5 mm/yr to 2.4 mm/yr, the deformation rate of mining area from -28.3 mm/yr to 3.7 mm/yr, the deformation rate of woodland areas from -21.3 mm/yr to 15.4 mm/yr, and the

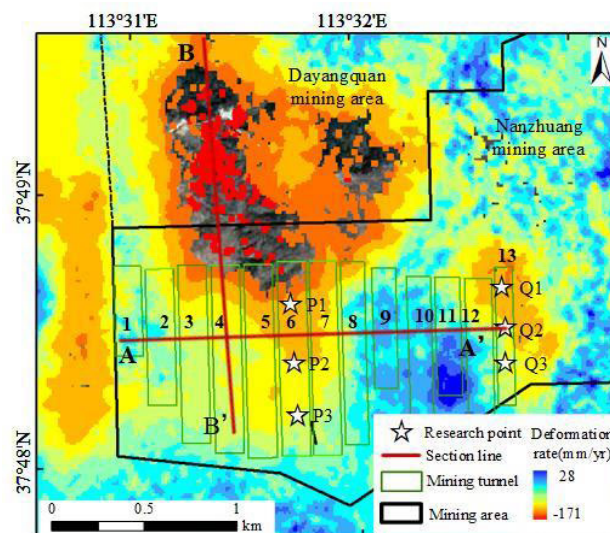


FIGURE 12. Southwest tunnels deformation rate map of Nanzhuang mine.

deformation rate of grassland ranges from -12.3 mm/yr to 13.0 mm/yr.

Because the larger deformation area is concentrated in the gangue pile and mining areas, the gangue pile and mining areas still need to be monitored continuously.

B. DEFORMATION AND MINING TUNNELS

The tunnel area is located in the southwest corner of the Nanzhuang mine and south of the Dayangquan mine. A total of 13 tunnels were closed after 2003, and the individual tunnels have sequential closing times, while the closing piece times of the individual tunnels are marked in Figure 11. The tunnels are named in order from west to east as tunnel 1 to 13. The closure times of tunnels 6 and 13 are December 2018 and June 2019, respectively. In this paper, we focus on the chronological analysis of these two closure tunnels (tunnels 6 and 13) and the comparative analysis of other tunnel selections. Figure 12 shows the regional deformation rate map of the mine tunnels, and the closure tunnels subsidence will still be partially affected by the Dayangquan mine. For the tunnel 6, which was closed in December 2018, and the tunnel 13, which was closed in June 2019, three characteristic points P1, P2, P3 and Q1, Q2, Q3 were selected for analysis. Their time-series deformation diagrams are shown in Figure 13(a) and 13(b). The other nine tunnels were selected from three points that were less affected by the northern mining areas, while the average value was taken for the time-series deformation analysis, and the results are shown in Figures 13(c) and 13(d).

The Figure13(a) shows that the active mining period for tunnel 6, which was closed in December 2018, began on April 2, 2018 and continued until December 25, 2018. The mining decline period runs from December 25, 2018, to the present. All three points P1, P2, and P3 show an inflection point on December 25, 2018. Consequently, all are clearly

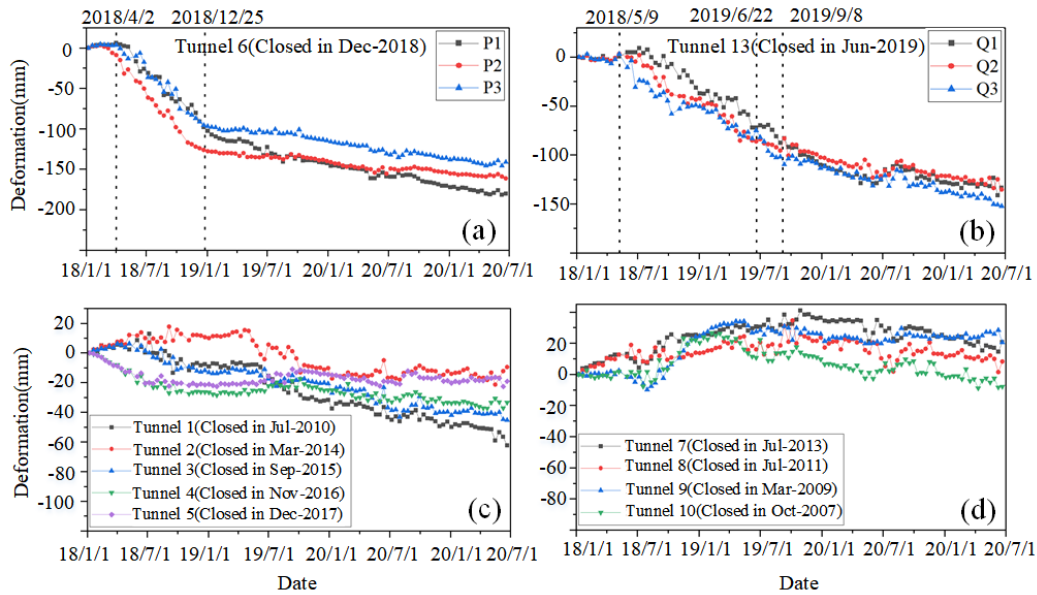


FIGURE 13. (a) Time-series displacement of selected points in Tunnel 6; (b) Time-series displacement of selected points in Tunnel 13; (c) Time-series displacement of selected points in Tunnel 1-5; (d) Time-series displacement of selected points in Tunnel 7-10.

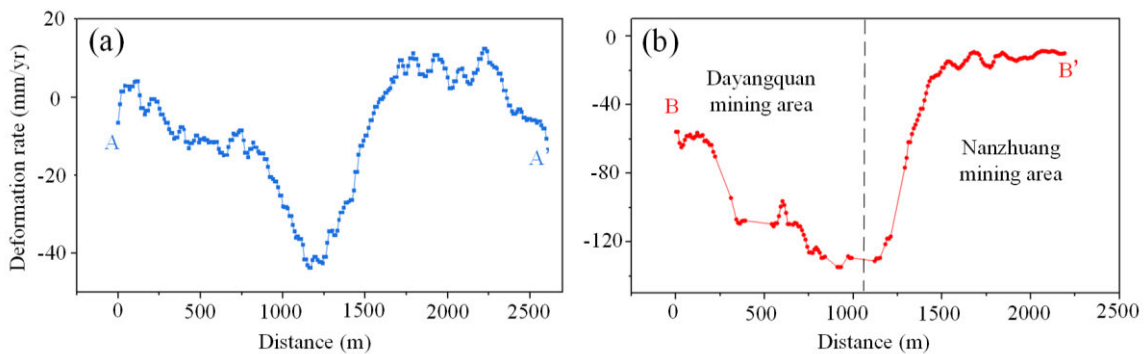


FIGURE 14. (a) Deformation rate map along A-A' profile, (b) Deformation rate map along B-B' profile.

in a flat state. The final cumulative deformation variables of the three points reach -180 mm, -162 mm, and -141 mm, respectively. While the time of the inflection point of the deformation of tunnel 6 corresponds to its closure time, which proves that the tunnel has a significant trend of slowing down after the closure and the mining area enters the decline period.

For tunnel 13, which was closed in June 2019, its active mining period was from May 9, 2018 to September 8, 2019, and the recession period was from September 8, 2019 to the present. Three points of Q1, Q2, and Q3 had delayed subsidence for more than two months from the closure of the tunnel in June 2019 and started to have a significant slowing trend on September 8, 2019. The cumulative deformation of the three points reached: -133 mm, -135 mm, and -152 mm.

Figures 13(c) and (d) show that from January 2018 to June 2021, the deformation is relatively stable for the remaining nine tunnels other than this one that was closed much earlier.

The five tunnels on the west side of tunnel 6 all experienced subsidence, with the maximum subsidence not exceeding 60 mm, while the four tunnels on the east side of tunnel 6 have some minor uplift, with the maximum uplift not exceeding 20 mm. These nine tunnels are relatively stable as they were closed earlier and are far away from the Dayangquan mine.

To study the spatial variation of the deformation of the mining areas, the spatial variation of the deformation of the mining areas was obtained along profiles A-A', and B-B', and the results are shown in Figure 14. From A-A', the surface deformation rate of the mining area increases, and then decreases. From the profile B-B', the further away from the mining area Dayangquan mine, the smaller the deformation rate. It can be presumed that the mining area Dayangquan mine has an impact on the surface subsidence for the closed mining areas, and the closer to the Dayangquan mine, the greater the impact and the greater the subsidence rate. The central tunnel is

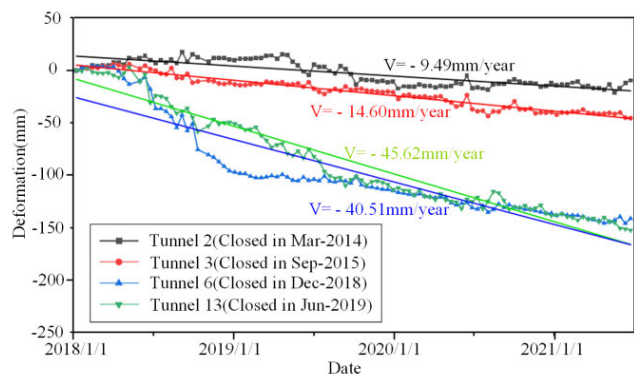


FIGURE 15. Relationship between surface deformation and the closed time of tunnels.

severer affected by the Dayangquan mine than the tunnels on either side, suggesting that the Dayangquan mine may be mined along the P1, P2, and P3 directions.

To investigate the relationship between closure time and deformation, four of the 13 tunnels were selected for analysis. Using the closing tunnel deformation as the vertical coordinate and the closing tunnel time as the horizontal coordinate, the scatter diagram of each of the four working faces is drawn, as shown in Figure 15. The Figure 15 shows that tunnel 6 and tunnel 13 have the shortest closing time, and the larger the subsidence rate, tunnel 2 has the longest closing time and the lowest subsidence rate. From tunnel 13 to tunnel 2, the slope of the corresponding curve gradually decreases, indicating that the longer the working face is closed, the smaller the surface deformation is, and the more the surface tends to be stable.

After time series deformation analysis, tunnels 6 and 13 have a significant tendency to slow subsidence after closure time, but overall accumulated subsidence is still significant. In addition, all tunnels are influenced by the Dayangquan mine in the north, and continued monitoring is always necessary for the tunnel area.

VI. CONCLUSION

In this paper, this method was used to monitor the deformation of the closed mining area, Nanzhuang mining areas, analyze the subsidence characteristic with the closure of the tunnel and the ground land use types, and assess the risk of subsidence in the closed mining areas. The conclusions are as follows:

(1) From January 8, 2018, to June 21, 2021, the overall deformation rate of the closed mining area in Yangquan Nanzhuang is -171 mm/yr to 28 mm/yr, and the cumulative deformation is -375 mm to 50 mm. The areas with larger deformation are mostly concentrated in the northeast area of the mine near the gangue pile, and the area adjacent to the Dayangquan mine in the closed mining areas.

(2) There are various types of features in the northeast direction within the closed mining areas of Nanzhuang, and

the subsidence is mainly concentrated in the gangue pile area and mining areas. Areas with high vegetation cover, such as woodland and grassland are stable areas with almost no deformation. Therefore, continued monitoring is still needed for gangue piles and mining areas where subsidence is high.

(3) Tunnel 6, which closed in December 2018, and tunnel 13, which closed in June 2019, continue to experience subsidence. Tunnel 6 has a significant slowing trend of subsidence after closure, tunnel 13 has a significant slowing trend of subsidence more than two months after closure, and the rest of the tunnels are at a stable stage at present. The rest of the tunnels are at a relatively stable stage.

(4) The high-risk areas of subsidence in the closed mining areas are concentrated in the vicinity of the gangue pile in the northeast area within the mine, and in the area bordering the closed mining areas and the northern part of the Dayangquan mine. This part of the area will affect the sustainable use of closed mining areas and require subsequent deformation monitoring.

ACKNOWLEDGMENT

The authors would like to thank the European Space Agency (ESA) for providing free and open Sentinel-1A data.

REFERENCES

- [1] R. Wang, M. Wang, Z. Zhang, T. Hu, J. Xing, Z. He, and X. Liu, "Geographical detection of urban thermal environment based on the local climate zones: A case study in Wuhan, China," *Remote Sens.*, vol. 14, no. 5, p. 1067, Feb. 2022.
- [2] Y. Li, J. Zhang, and Y. Luo, "Land subsidence in Beijing City from InSAR time series analysis with small baseline subset," *Geomatics Inf. Sci. Wuhan Univ.*, vol. 38, no. 11, pp. 1374–1377, 2013.
- [3] W. Yunjia, "Research progress and prospect on ecological disturbance monitoring in mining area," *Acta Geodaetica et Cartographica Sinica*, vol. 46, no. 10, p. 1705, 2017.
- [4] G. He, *Mining Subsidence Theory*. Xuzhou, China: China Univ. Mining & Technology, 1991, p. 375.
- [5] X. Yong, W. Chen, Y. Wu, Y. Tao, J. Zhou, and J. He, "A two-stage framework for site selection of underground pumped storage power stations using abandoned coal mines based on multi-criteria decision-making method: An empirical study in China," *Energy Convers. Manag.*, vol. 260, May 2022, Art. no. 115608.
- [6] R. Wenjing, J. Hongguo, and Y. Bin, "Monitoring and parameter inversion of ground subsidence in mining area based on SBAS-InSAR method," *Bull. Surveying Mapping*, vol. 3, p. 113, Jan. 2021.
- [7] L. Wu, H. Gong, X. Zhao, P. Fan, B. Wu, and Y. Zhou, "Deformation monitoring and analysis of Yangquan mining area based on DInSAR technology," *Coal Mine Saf.*, vol. 49, no. 7, pp. 193–197, 2018.
- [8] K. D. Kim, S. Lee, H. J. Oh, J. K. Choi, and J. S. Won, "Assessment of ground subsidence hazard near an abandoned underground coal mine using GIS," *Environ. Geol.*, vol. 50, no. 8, pp. 1183–1191, 2006.
- [9] G. Liu, L. Zhang, S. Cheng, and T. Jiang, "Feasibility analysis of monitoring mining surface substance using InSAR GPS data fusion," (in Chinese), *Bull. Surveying Mapping*, no. 11, pp. 10–13, 2005.
- [10] M. Chini, R. Pelich, L. Pulvirenti, N. Pierdicca, R. Hostache, and P. Matgen, "Sentinel-1 InSAR coherence to detect floodwater in urban areas: Houston and hurricane Harvey as a test case," *Remote Sens.*, vol. 11, p. 107, Jan. 2019.
- [11] Y. Fengyu and S. Jingwen, "Attribution analysis on land subsidence feature in Hexi area of Nanjing by InSAR and geological data," *Geomatics Inf. Sci. Wuhan Univ.*, vol. 45, no. 3, pp. 442–450, 2020.
- [12] A. Ferretti, A. Fumagalli, F. Novali, C. Prati, F. Rocca, and A. Rucci, "A new algorithm for processing interferometric data-stacks: SqueeSAR," *IEEE Trans. Geosci. Remote Sens.*, vol. 49, no. 9, pp. 3460–3470, Sep. 2011.

- [13] Z. W. Li, W. B. Xu, G. C. Feng, J. Hu, C. C. Wang, X. L. Ding, and J. J. Zhu, "Correcting atmospheric effects on InSAR with MERIS water vapour data and elevation-dependent interpolation model," *Geophys. J. Int.*, vol. 189, no. 2, pp. 898–910, May 2012.
- [14] L. Xiao, "Time series subsidence analysis of drilling solution mining rock salt mines based on Sentinel-1 data and SBAS-InSAR technique," *Int. J. Remote Sens.*, vol. 23, pp. 501–513, Jan. 2019.
- [15] P. Ma, H. Lin, W. Wang, H. Yu, F. Chen, L. Jiang, L. Zhou, Z. Zhang, G. Shi, and J. Wang, "Toward fine surveillance: A review of multitemporal interferometric synthetic aperture radar for infrastructure health monitoring," *IEEE Geosci. Remote Sens. Mag.*, vol. 10, no. 1, pp. 207–230, Mar. 2022.
- [16] Z. Zhang, H. Lin, M. Wang, X. Liu, Q. Chen, C. Wang, and H. Zhang, "A review of satellite synthetic aperture radar interferometry applications in permafrost regions: Current status, challenges, and trends," *IEEE Geosci. Remote Sens. Mag.*, vol. 10, no. 3, pp. 93–114, Sep. 2022.
- [17] X. Liu, X. Xing, D. Wen, L. Chen, Z. Yuan, B. Liu, and J. Tan, "Mining-induced time-series deformation investigation based on SBAS-InSAR technique: A case study of drilling water solution rock salt mine," *Sensors*, vol. 19, no. 24, p. 5511, Dec. 2019.
- [18] J. Liu, "Underground coal fires identification and monitoring using time-series InSAR with persistent and distributed scatterers: A case study of Miquan coal fire zone in Xinjiang, China," *IEEE Access*, vol. 7, pp. 164492–164506, 2019.
- [19] X. Diao, K. Wu, R. Chen, and J. Yang, "Identifying the cause of abnormal building damage in mining subsidence areas using InSAR technology," *IEEE Access*, vol. 7, pp. 172296–172304, 2019.
- [20] H. Fan, X. Gao, J. Yang, K. Deng, and Y. Yu, "Monitoring mining subsidence using a combination of phase-stacking and offset-tracking methods," *Remote Sens.*, vol. 7, no. 7, pp. 9166–9183, 2015.
- [21] Q. He, Y. Zhang, H. Wu, and Y. Luo, "Mining subsidence monitoring with modified time-series SAR interferometry method based on the multi-level processing strategy," *IEEE Access*, vol. 9, pp. 106039–106048, 2021.
- [22] D. Chen, H. Chen, W. Zhang, C. Cao, K. Zhu, X. Yuan, and Y. Du, "Characteristics of the residual surface deformation of multiple abandoned mined-out areas based on a field investigation and SBAS-InSAR: A case study in Jilin, China," *Remote Sens.*, vol. 12, no. 22, p. 3752, Nov. 2020.
- [23] L. Bateson, F. Cigna, D. Boon, and A. Sowter, "The application of the Intermittent SBAS (ISBAS) InSAR method to the South Wales Coalfield, U.K.," *Int. J. Appl. Earth Observ. Geoinf.*, vol. 34, pp. 249–257, Feb. 2015.
- [24] L. Li, C. Zhao, J. Huang, C. Huan, H. Wu, P. Xu, L. Yuan, and Y. Chen, "Complex surface deformation of the coalfield in the northwest suburbs of Xuzhou from 2015 to 2020 revealed by time series InSAR," *Can. J. Remote Sens.*, vol. 47, no. 5, pp. 697–718, Sep. 2021.
- [25] B. Chen, H. Yu, X. Zhang, Z. Li, J. Kang, Y. Yu, J. Yang, and L. Qin, "Time-varying surface deformation retrieval and prediction in closed mines through integration of SBAS InSAR measurements and LSTM algorithm," *Remote Sens.*, vol. 14, no. 3, p. 788, Feb. 2022.
- [26] C. Huang, H. Xia, and J. Hu, "Surface deformation monitoring in coal mine area based on PSI," *IEEE Access*, vol. 7, pp. 29672–29678, 2019.
- [27] Z. Zhang, C. Wang, Y. Tang, H. Zhang, and Q. Fu, "Analysis of ground subsidence at a coal-mining area in Huainan using time-series InSAR," *Int. J. Remote Sens.*, vol. 36, pp. 5790–5810, 2015.
- [28] A. H.-M. Ng, L. Ge, Z. Du, S. Wang, and C. Ma, "Satellite radar interferometry for monitoring subsidence induced by longwall mining activity using Radarsat-2, Sentinel-1 and ALOS-2 data," *Int. J. Appl. Earth Observ. Geoinf.*, vol. 61, pp. 92–103, Sep. 2017.
- [29] P. Berardino, G. Fornaro, R. Lanari, and E. Sansosti, "A new algorithm for surface deformation monitoring based on small baseline differential SAR interferograms," *IEEE Trans. Geosci. Remote Sens.*, vol. 40, no. 11, pp. 2375–2383, Nov. 2002.
- [30] D. Li, K. Deng, X. Gao, and H. Niu, "Monitoring and analysis of surface subsidence in mining area based on SBAS-InSAR," *Geomatics Inf. Sci. Wuhan Univ.*, vol. 43, no. 10, pp. 1531–1537, 2018.
- [31] M. Costantini, "A novel phase unwrapping method based on network programming," *IEEE Trans. Geosci. Remote Sens.*, vol. 36, no. 3, pp. 813–821, May 1998.
- [32] Y. Aimaiti, F. Yamazaki, W. Liu, and A. Kasimu, "Monitoring of land-surface deformation in the Karamay oilfield, Xinjiang, China, using SAR interferometry," *Appl. Sci.*, vol. 7, no. 8, p. 772, Jul. 2017.
- [33] G. Chen, Y. Zhang, R. Zeng, Z. Yang, X. Chen, F. Zhao, and X. Meng, "Detection of land subsidence associated with land creation and rapid urbanization in the Chinese loess plateau using time series InSAR: A case study of Lanzhou new district," *Remote Sens.*, vol. 10, no. 2, p. 270, Feb. 2018.
- [34] B. Hu, J. Zhou, J. Wang, Z. Chen, D. Wang, and S. Xu, "Risk assessment of land subsidence at Tianjin coastal area in China," *Environ. Earth Sci.*, vol. 59, no. 2, pp. 269–276, Nov. 2009, doi: [10.1007/s12665-009-0024-6](https://doi.org/10.1007/s12665-009-0024-6).
- [35] J. F. Aceves-Quesada, J. Díaz-Salgado, and J. López-Blanco, "Vulnerability assessment in a volcanic risk evaluation in Central Mexico through a multi-criteria-GIS approach," *Natural Hazards*, vol. 40, no. 2, pp. 339–356, Jan. 2007, doi: [10.1007/s11069-006-0018-6](https://doi.org/10.1007/s11069-006-0018-6).
- [36] C. Jiang, L. Wang, and X. Yu, "Retrieving 3D large gradient deformation induced to mining subsidence based on fusion of Boltzmann prediction model and single-track InSAR earth observation technology," *IEEE Access*, vol. 9, pp. 87156–87172, 2021.



ZHEN LI is a Senior Engineer, a Registered Surveying and Mapping Engineer, and currently the Director of the Ecological Environment Center, Shanxi Coal Geological and Geophysical Surveying and Mapping Institute of Shanxi Province. He has been engaged in surveying and mapping geographic information, ecological environmental protection and restoration for nine years, and has been the person in charge of 18 surveying and mapping geographic information and ecological restoration projects. He has received five utility model patents and published eight academic papers.



ZHONGBIN TIAN is a Senior Engineer and currently a member of the Party Committee and the Deputy General Manager of Shanxi Geological Group Company Ltd. He also serves as the Party Committee Secretary and the Chairperson for the Shanxi Coal Geological and Geophysical Exploration and Mapping Institute of Shanxi Province. He has been engaged in geophysical exploration and research of coal and coal-derived gas for 23 years. His six invention patents, ten utility model patents, and five software copyrights were authorized. He has published one monograph and 33 academic papers, including three SCI source journals and four EI source journals.



BIN WANG received the bachelor's degree in exploration technology and engineering and the master's degree in geological resources and geological engineering from the Hebei University of Engineering. He worked with the Coal Geological Geophysical Exploration Surveying and Mapping Institute of Shanxi Province, in 2015. He has published two academic papers. His research interests include geological disaster prevention and control, ecological restoration, mineral geology, mine water prevention and control, and natural resources survey monitoring and confirmation of professional.



QIHAO CHEN received the B.E. degree in geographic information system and the M.E. and Ph.D. degrees in cartography and geographic information engineering from the China University of Geosciences (CUG), Wuhan, China, in 2004, 2007, and 2011, respectively. He is currently an Associate Professor with the School of Geography and Information Engineering, CUG. His research interest includes polarimetric.



WEIBING LI received the bachelor's degree. He worked with Shanxi Coal Geological Investigation and Research Institute Company Ltd. He is an engineer. His research interest includes mine geological mapping research.



ZHENGJIA ZHANG received the B.Sc. degree in geoscience information system from the Hefei University of Technology, Hefei, China, in 2012, and the Ph.D. degree in microwave remote sensing from the Institute of Remote Sensing and Digital Earth, Chinese Academy of Sciences, Beijing, China, in 2017.

He is currently an Associate Professor with the School of Geography and Information Engineering, China University of Geosciences, Wuhan, China. His research interests include synthetic aperture radar (SAR) interferometric technique, time-series interferometric SAR, and their applications on nature hazards and permafrost region.

...